Atmos. Chem. Phys., 23, 4343–4359, 2023
https://doi.org/10.5194/acp-23-4343-2023

Atmospheric Chemistry and Physics
Open Access
EGU

Research article

High frequency of new particle formation events driven by summer monsoon in the central Tibetan Plateau, China

Lizi Tang[1], Min Hu[1,2], Dongjie Shang[1], Xin Fang[1], Jianjiong Mao[2], Wanyun Xu[3], Jiacheng Zhou[4], Weixiong Zhao[4], Yaru Wang[1], Chong Zhang[1], Yingjie Zhang[5], Jianlin Hu[2], Limin Zeng[1,2], Chunxiang Ye[1], Song Guo[1,2], and Zhijun Wu[1,2]

[1]State Key Joint Laboratory of Environmental Simulation and Pollution Control, International Joint Laboratory for Regional Pollution Control, Ministry of Education (IJRC), College of Environmental Sciences and Engineering, Peking University, Beijing, 100871, China
[2]Collaborative Innovation Center of Atmospheric Environment and Equipment Technology, Jiangsu Key Laboratory of Atmospheric Environment Monitoring and Pollution Control, Nanjing University of Information Science & Technology, Nanjing, 210044, China
[3]State Key Laboratory of Severe Weather & Key Laboratory for Atmospheric Chemistry of CMA, Institute of Atmospheric Composition, Chinese Academy of Meteorological Sciences, Beijing, 100081, China
[4]Laboratory of Atmospheric Physico-Chemistry, Anhui Institute of Optics and Fine Mechanisms, HFIPS, Chinese Academy of Science, Hefei, 230031, Anhui, China
[5]School of Ecology and Nature Conservation, Beijing Forestry University, Beijing, 100083, China

Correspondence: Min Hu (minhu@pku.edu.cn)

Received: 18 June 2022 – Discussion started: 13 September 2022
Revised: 30 November 2022 – Accepted: 14 March 2023 – Published: 13 April 2023

Abstract. New particle formation (NPF) is an important source of cloud condensation nuclei (CCN), which affects Earth's radiative balance and global climate. The mechanism and CCN contribution of NPF at the high-altitude mountains, especially in the Tibetan Plateau (TP), was unclear due to lack of measurements. In this study, intensive measurements were conducted at the Nam Co station (4730 m a.s.l.) in the central TP during both the pre-monsoon and summer monsoon seasons. The frequencies of NPF events exhibited evident seasonal differences with 15 % in the pre-monsoon season and 80 % in the monsoon season. The comprehensive analysis of the measured condensation sink (CS), gaseous precursors and meteorological conditions, supplemented by the model simulations of SO_2 and volatile organic compound (VOC), points to the organic involved nucleation as the dominant mechanism. Condensation sink and gaseous sulfuric acid could have no significant effect on the occurrence of NPF events. The frequent NPF events in the summer monsoon season may result from the higher frequency of southerly and southwesterly air masses, which brought the organic precursors to participate in the NPF process. It had increased the aerosol number concentrations and CCN at supersaturation of 1.2 % by more than 2 and 0.6 times compared with those in the pre-monsoon season, respectively. Considering that the smaller particles formed by NPF may further grow and reach CCN size during the following days due to the low-level coagulation sink, the amount of potential CCN in the monsoon season could be much larger than our local measurement results. Our results emphasized the importance of considering the seasonal effect of NPF when simulating the amounts of aerosols and CCN in the high-altitude atmosphere. Long-term investigations with a full set of instrumentation are required for deeper scientific understanding of NPF process and its role in the global budget in the TP.

Published by Copernicus Publications on behalf of the European Geosciences Union.

1 Introduction

Atmospheric aerosols can affect Earth's radiative balance through direct interaction with solar radiation and by serving as cloud condensation nuclei (CCN), and thus they can affect global climate. There is considerable uncertainty about the total radiative forcing contributed by aerosol particles, mainly from the number concentrations and sizes of CCN (IPCC, 2021). New particle formation (NPF) is a physical and chemical process, comprising nucleation of gaseous precursors and the subsequent growth of the nucleated clusters into aerosol particles. NPF has been considered to be an important source of aerosols and contributes a major fraction to the global CCN budget. Model simulations found that up to 45 % of global CCN were secondary aerosols derived from NPF process, with a large fraction created in the free troposphere (Merikanto et al., 2009). Furthermore, NPF may be more important to the total CCN budget in the pristine atmosphere than that in the industrial atmosphere (Gordon et al., 2017). Similarly, the field observations in diverse atmospheric environmental showed the more significant CCN contribution from NPF events in pristine atmosphere, especially in high-altitude mountains (Kerminen et al., 2018).

The Tibetan Plateau (TP) is the largest plateau in China and the highest plateau in the world, with an average altitude of over 4000 m a.s.l. It is known as the "roof of the world" and "the third pole" of the Earth and plays a fundamental role in the regional climate and environment through various dynamic and thermal effects (Yanai and Wu, 2006). Due to the rare anthropogenic activities, the TP is considered one of the most pristine locations around the world and an ideal location for observations of free-tropospheric air masses and NPF events. However, there have been few NPF studies in the TP, mainly due to the challenges in measuring particle numbers and precursors under the adverse meteorological and topographic conditions such as the extremely low temperature, the thin air and the steep mountains. Several long-term and short-term observations have been conducted in different regions of the TP in recent years. A significant seasonal variation of NPF frequency was observed in the TP. For example, the long-term NPF measurement at Himalayan Nepal Climate Observatory at Pyramid (NCO-P) site on the southern TP showed the distinct NPF frequency in the different seasons with the highest in the monsoon period (Venzac et al., 2008). The occurrence of NPF events in NCO-P was initiated by the up-valley winds which sent the biogenic condensable vapors from Khumbu valley to the high-altitude location (Bianchi et al., 2021). At Mt. Yulong on the southeastern TP, the NPF frequency was only 14 % during the pre-monsoon season and the occurrence of NPF events was related to an elevated boundary layer or transported biomass burning pollutants from southern Asia, but not to biogenic condensable vapors (Shang et al., 2018; Du et al., 2015). For Mt. Daban on the northeastern TP, the high frequency of NPF events was observed during the post-monsoon season (80 %) (Du et al., 2015). These results indicated that the frequency and mechanism of NPF may be associated with air mass origins and monsoon shift in the southern, southeastern and northeastern TP. However, there were few NPF studies conducted in the central TP especially for the reaction of NPF on the monsoon season shifting in this region.

In this study, intensive measurements during the pre-monsoon and monsoon seasons were conducted at the Nam Co station (4730 m a.s.l.) in the central TP, which can better represent the regional characteristics of TP. Collocated measurements, including particle number size distributions (PNSDs), trace gases and meteorological parameters, and assisted Weather Research and Forecasting (WRF) and Community Multiscale Air Quality (CMAQ) models were employed to investigate the characteristics of PNSDs and NPF events. This study aimed to (1) characterize NPF events in the pre-monsoon and summer monsoon season in the central TP, (2) investigate the source of the NPF events occurrence in the pre-monsoon and summer monsoon season in the central TP, and (3) quantify the CCN contribution of NPF in the pre-monsoon and summer monsoon season in the central TP.

2 Material and methods

2.1 Measurement site

An intensive field campaign was carried out at a high mountain observatory at the central Tibetan Plateau, i.e., the Nam Co station (30.8° N, 91.0° E; 4730 m a.s.l.) during the in-depth study of the atmospheric chemistry over the Tibetan Plateau in the year of 2019, referred to as @Tibet 2019 field campaign (Fig. 1). The Nam Co station is located near Nam Co Lake (area: 1920 km^2), the highest and largest saltwater lake in the world. which is backed by the Nyenchen Tanglha Mountains in the south. The ecology of the surrounding area is semi-arid land dominated by alpine meadow and barren areas. The capital city (Lhasa) of the Tibet Autonomous Region is about 100 km southeast of the station. The closest town, Dangxiong, is about 70 km southeast of the station, between which are the Nyenchen Tanglha Mountains. Overall, the Nam Co station is located in a typical pristine environment and there are almost no local anthropogenic source emissions in this area. The measurements were conducted from 26 April to 22 May 2019 and 15 to 25 June 2019 and can be representative of the pre-monsoon season and the summer monsoon season, respectively (Sect. S1) (Bonasoni et al., 2010; Cong et al., 2015).

2.2 Instruments and methods

The sampling was conducted at the observatory field of the Nam Co station (Fig. 1c). O_3 was detected using ultraviolet (UV) absorption by a "Model 49C Ozone Analyzer" (Thermo Scientific, USA). CO and water content (H_2O) were measured by Picarro G2401 based on cavity ring-down spec-

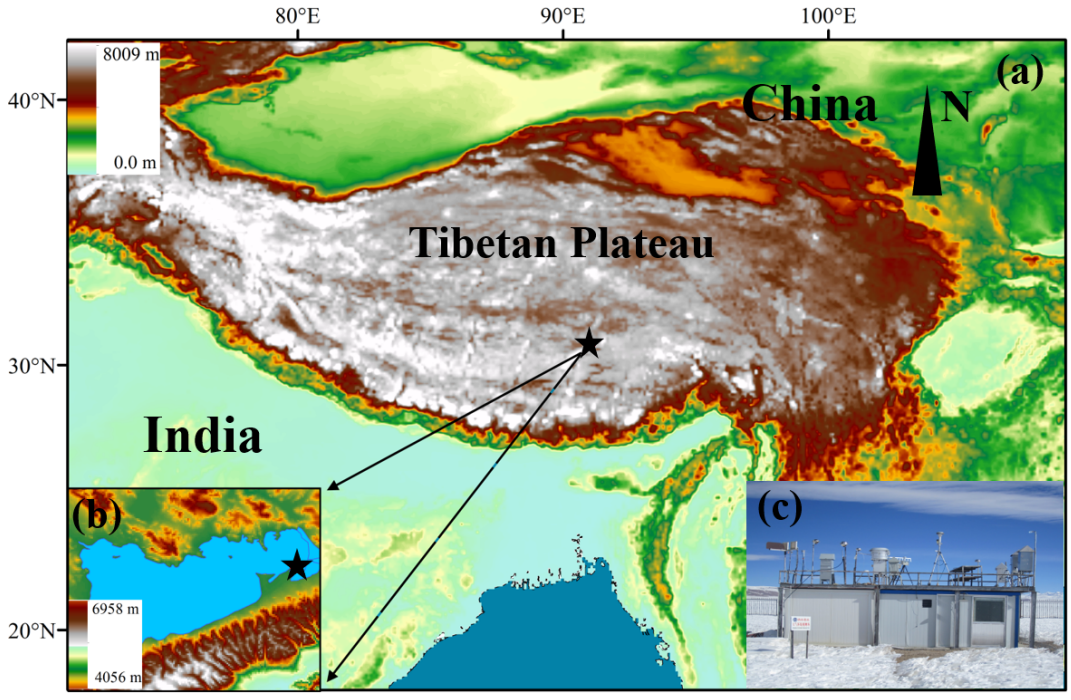

Figure 1. Location map for **(a)** the Tibetan Plateau, **(b)** the Nam Co station, colored according to altitude. **(c)** The appearance drawing of atmospheric environment observatory field of the Nam Co station (Yin et al., 2021).

troscopy. Meteorological parameters including wind speed (WS), wind direction (WD), temperature (T) and relative humidity (RH) were measured by the automatic meteorological station (Met One Instrument Inc). The photolysis frequencies of O_3 (JO^1D) were monitored using a spectral radiometer (ultra-fast CCD-detector spectrometer, METCON GmbH, Germany); 99 types of volatile organic compounds (VOCs) were measured by an online gas chromatograph coupled with a mass spectrometer and flame ionization detectors (GC-MS/FID) (TH-PKU 300B, Wuhan Tianhong Instrument Co. Ltd., China) in the pre-monsoon season (Wang et al., 2014). Black carbon (BC) was measured with an Aethalometer (Magee Scientific, model AE33), and the concentration of BC at 880 nm was used in this study to reduce the influence of brown carbon (Kirchstetter et al., 2004).

PNSDs in the stokes size range of 4 and 700 nm were obtained by integrating two sets of scanning mobility particle spectrometers (SMPSs). The first SMPS measured particles with the size of 4–45 nm, consisting of a TSI Model 3085 DMA and a TSI Model 3776 CPC (with a flow rate of 1.5 L min^{-1}). The second SMPS measured particles with the size of 45–700 nm, consisting of a TSI Model 3081 DMA and a TSI Model 3775 CPC (with a flow rate of 0.3 L min^{-1}). A silicon diffusion tube was placed before the SMPS, which kept the relative humidity (RH) of the sampling air under 40 %. PNSDs were corrected for particle losses in the SMPS and the sampling tube, following the method of "equivalent pipe length" as described in Wiedensohler et al. (2012).

To reveal the transport pathway of air masses that arrive at the site, the 48 h backward trajectories of the air mass at 500 m above the ground (5230 m a.s.l.) were computed using the HYSPLIT (Hybrid Single Particle Lagrangian Integrated Trajectory) model and Global Data Assimilation System (GDAS) data.

2.3 Model simulation

Considering the limited measurements on SO_2 and VOC in this observation (only VOC during the pre-monsoon season), Weather Research and Forecasting/Community Multiscale Air Quality (WRF/CMAQ) modeling system was adopted to simulate the level of SO_2 and VOC in the whole observation period, to assist in the analysis of the role of sulfuric acid and organics in NPF events.

The Weather Research and Forecasting (WRF) (version 4.2.1) model was used to simulate the meteorological conditions with the FNL (Final) reanalysis dataset. The 6 h FNL data were obtained from the U.S. National Center for Atmospheric Research (NCAR), with a spatial resolution of 1.0° × 1.0° (http://rda.ucar.edu/datasets/ds083.2/, last access: 28 April 2022). The Community Multiscale Air Quality version 5.3.2 (CMAQv5.3.2) model, being one of the three-dimensional chemical transport models (CTMs) (Appel et al., 2021), configured with the gas-phase mechanism of SAPRC07tic and the aerosol module of AERO6i, was employed in this study to simulate the air quality over Tibet in the observation period (26 April to 22 May and 15 to 25 June

in 2019). Air quality simulations were performed with a horizontal resolution of 12 km. The corresponding domain covered Tibet and the surrounding countries and regions with 166×166 grids (Fig. S2), with the 18 layers in vertical resolution. Detailed information about the model setting is provided in Sect. S2.

The Multi-resolution Emission Inventory for China version 1.3 (MEICv1.3) (http://www.meicmodel.org, last access: 1 June 2022) and Regional Emission inventory in ASia (REASv3.2) (https://www.nies.go.jp/REAS/, last access: 1 June 2022) were used to provide the anthropogenic emissions from China and neighboring countries and regions, respectively. The MEICv1.3 emissions of the year 2019 were used. For REAS, the emission inventory in the year 2015 was used for 2019 as no emission inventory was released for the years after 2015. Although emission inventories are usually released 3 years behind, we acknowledge that this may cause additional uncertainties in the simulation. Biogenic emissions were generated using the Model for Emissions of Gases and Aerosols from Nature (MEGANv2.1) (Guenther et al., 2012). The open biomass burning emissions were processed using the Fire Inventory for NCAR (FINN) during the entire study period (Wiedinmyer et al., 2011).

The model evaluation is introduced in Sect. S2. The WRF and CMAQ models successfully reproduced the meteorological fields and air pollutants including PM and O_3 with model performance indices meeting the suggested benchmarks. For VOC, the observed VOC and predicted VOC in the pre-monsoon season were compared to examine the model performance. The benchmarks for VOC had not been reported, but the statistical metrics of MFB (mean fractional bias, -0.47) and MFE (mean fractional error, 0.49) in this study are within the range reported in previous VOC modeling results (Hu et al., 2017). The correlation coefficient (R) between simulated and observed VOC is 0.41, which reflected that the model can fairly simulate the variation of VOC concentration. It should be noted that VOC was underpredicted on the whole, which may due to the uncertainty of the emission inventory as mentioned before. For SO_2, the WRF/CMAQ models have been successfully reproduced SO_2 in major regions in China with R of 0.25–0.79 (Mao et al., 2022). And the WRF/CMAQ models achieved good performance in simulating SO_2 at Mt. Yulong on the southern TP (Sect. S2). Here, the simulated SO_2 level in the model domain is comparable with that measured at Mt. Yulong (Shang et al., 2018), with average values of 0.03 ± 0.02 and 0.06 ± 0.05 ppbv. At the same time, considering that both BC and SO_2 are mainly emitted from coal combustion and biomass burning, BC could be a good indicator for SO_2 especially for pristine environment without local anthropogenic source emissions. As shown in Fig. S7, a good correlation between SO_2 and BC measured at Mt. Yulong was found with correlation coefficient (R) of 0.79 (Shang et al., 2018). In this study, the modeled SO_2 and measured BC also showed good correlation with R of 0.58 (Fig. S8). In general, the results of model simulation showed good performance in statistical parameters and correlation analysis with other tracers. The modeled VOC and SO_2 may be helpful for the NPF analysis.

2.4 Parameterization of NPF

In this study, a typical NPF event was defined by a burst in the 3–10 nm particle number concentration (PN_{3-10}) and subsequent growth of these newly formed particles (Fang et al., 2020; Dal Maso et al., 2005). The days without newly particle formation were defined as non-event days. Days in which the increase of PN_{3-10} was observed without the particles growing to the larger size or days in which the later phase of a mode growing in the Aitken mode size range can be observed were treated as undefined days (Dal Maso et al., 2005). The examples of the classification of NPF events are shown in Fig. S9.

During the NPF events, the formation rate was calculated using the following formula (Cai and Jiang, 2017):

$$\begin{aligned} J_{d_k} = {} & \frac{\mathrm{d}N_{[d_k,d_\mathrm{u})}}{\mathrm{d}t} + \sum_{d_g=d_k}^{d_\mathrm{u}-1} \sum_{d_i=d_\mathrm{min}}^{+\infty} \\ & \cdot \beta_{(i,g)} N_{[d_i,d_{i+1})} N_{[d_g,d_{g+1})} \\ & - \frac{1}{2} \sum_{d_g=d_\mathrm{min}}^{d_\mathrm{u}-1} \sum_{d_i^3=\max(d_\mathrm{min}^3,d_k^3-d_\mathrm{min}^3)}^{d_{i+1}^3+d_{g+1}^3 \le d_\mathrm{u}^3} \\ & \cdot \beta_{(i,g)} N_{[d_i,d_{i+1})} N_{[d_g,d_{g+1})} \\ & + n_\mathrm{u} \cdot \mathrm{GR}_\mathrm{u} \end{aligned} , \quad (1)$$

where J_{d_k} is the formation rate of particles at size d_k, and d_u is the upper size bound of the target size range. Here d_k and d_u are selected to be 4 and 25 nm, respectively. $N_{[d_k,d_\mathrm{u})}$ is the total number concentration of particles in the diameters of $[d_k d_\mathrm{u})$. d_i is the lower bound of each measured size bin, and d_min is lowest size limit detected by measuring instrument. $\beta_{(i,g)}$ is the coagulation coefficient for the collision between the particle at size of d_i and the particle at size of d_g. n_u is the particle size distribution function ($\mathrm{d}N/\mathrm{d}d_\mathrm{p}$). GR_u is the growth rate at size of d_u.

The growth rate (GR) was obtained by the mode-fitting method described in Dal Maso et al. (2005). In short, the PNSDs during NPF event days were fitted as the sum of three-mode lognormal distribution. GR was calculated as the variation of the geometric mean diameter D_m of newly formed mode (4–25 nm) in unit internal (Dal Maso et al., 2005):

$$\mathrm{GR} = \frac{\Delta D_\mathrm{m}}{\Delta t}. \quad (2)$$

To evaluate the scavenging effects of preexisting particles on condensable vapors, the condensation sink (CS) was calculated as follows (Dal Maso et al., 2005):

$$\mathrm{CS} = 2\pi D \sum \beta_\mathrm{m}\left(D_{\mathrm{p},i}\right) D_{\mathrm{p},i} N_i, \quad (3)$$

where D is the diffusion coefficient of the condensing vapor, β_m is the transition regime correction factor, and $D_{p,i}$ and N_i are the diameter and number concentration in the size class i, respectively.

2.5 Calculation of CCN concentration

The CCN number concentration was calculated based on the assumption that particles larger than a certain diameter could act as CCN. The critical diameter (D_c) of the CCN activation at the supersaturation (S_c) can be calculated based on κ-Köhler theory (Petters and Kreidenweis, 2007):

$$\kappa = \frac{4A^3}{27D_c^3 \ln^2 S_c} \quad (4)$$

$$A = \frac{4\sigma_{s/a}M_w}{RT\rho_w}, \quad (5)$$

where κ is the hygroscopicity parameter about the composition dependence of the solution water activity. $\sigma_{s/a}$ is the water surface tension ($0.0728\,N\,m^{-1}$). M_w and ρ_w are the molecular weight and density of water, respectively. R is the universal gas constant ($J\,mol^{-1}\,K^{-1}$), and T is the absolute temperature (K).

3 Results and discussions

3.1 Characteristics of meteorology and atmospheric pollutants

The distinct meteorological characterizations were exhibited in the two seasons. As shown in Figs. 2 and S10, the temperature behavior was characterized by higher values in the monsoon season (10.4 ± 4.1 °C) and lower values in the pre-monsoon season (3.1 ± 3.6 °C) with an average value of 5.3 ± 5.1 °C. The relative humidity (RH) seems very similar in the two seasons (50 ± 21 % in the pre-monsoon season vs. 48 ± 19 % in the monsoon season), but the water content (H_2O) in the air during the monsoon season (1.0 ± 0.2 %) was clearly higher than that in the pre-monsoon season (0.6 ± 0.2 %), which reflected the wetter environment in the monsoon period. The wind speed (WS) was comparable during the two seasons, which was $4.2 \pm 2.7\,m\,s^{-1}$ in the pre-monsoon season and $4.5 \pm 2.7\,m\,s^{-1}$ in the monsoon season, respectively. The wind direction (WD) showed a clear divergence, with westerly and southwesterly winds prevailing in the pre-monsoon season, and southerly winds prevailing in the monsoon season (Fig. S11). The frequencies of air masses arriving at the observation station from various directions during the two seasons are shown in Fig. S12. In the pre-monsoon season, strong westerlies pass through western Nepal, northwestern India and Pakistan (i.e., southern Himalayas). In the monsoon season, air masses were more derived from Bangladesh and northeastern India and brought moisture that originated in the Bay of Bengal. The seasonality of meteorology was generally in agreement with the previous studies in the TP, which is strongly influenced by the large-scale Asian monsoon circulation (Cong et al., 2015; Bonasoni et al., 2010).

As a background high-altitude site on the TP, the Nam Co station displayed a low particle concentration. On average $PM_{0.8}$ was $1.8 \pm 1.0\,\mu g\,m^{-3}$, which was similar to PM_1 ($2\,\mu g\,m^{-3}$) measured by a high-resolution time-of-flight aerosol mass spectrometer at the Nam Co station in 2015 (J. Xu et al., 2018). The particulate matter concentration at the Nam Co station was lower than the PM_1 observed at Qomolangma Station ($4.4\,\mu g\,m^{-3}$) on the southern TP and Waliguan Observatory ($9.1\,\mu g\,m^{-3}$) on the northeastern TP, which resulted from a much longer transport distance of anthropogenic emissions compared with Qomolangma Station and Waliguan Observatory (Zhang et al., 2021). The average concentration of BC was $223 \pm 135\,ng\,m^{-3}$ during the whole measurement period, which is comparable with previous observations (J. Xu et al., 2018, 2020; Wang et al., 2016; R. Xu et al., 2018), and represents the background level in the TP region. The average O_3 concentration was 58 ± 15 ppbv, which was similar to the results from some high-elevation sites in the TP (Bonasoni et al., 2010; Shang et al., 2018) and higher than the results from Beijing during spring (Chen et al., 2020). Consistent with previous research (J. Xu et al., 2018; Cong et al., 2015; Yin et al., 2021), higher PM, BC and O_3 concentrations were found during the pre-monsoon season (Fig. S13). The higher BC and PM may result from the active biomass-burning emissions in the pre-monsoon season on the southern TP (Cong et al., 2015). The higher O_3 concentrations in the pre-monsoon season were primarily attributed to stratospheric intrusion of ozone (Yin et al., 2021). In contrast, there was no noticeable difference in CO between the two seasons, and the average concentration was 0.12 ± 0.14 ppmv.

3.2 Higher frequency of new particle formation in the monsoon season

Figure 2g shows the evolution of PNSD for the entire study. It can be seen that NPF events in the monsoon period were observed almost every day (8 NPF days and 2 undefined days, 80 %), while the frequency of NPF events was extremely low during the pre-monsoon period (4 in 27 d, 15 %). As shown in Table 1, the event frequency at the Nam Co station during the monsoon season was higher than the result reported at NCO-P site on the southern TP in the monsoon season (57 %) (Venzac et al., 2008), and similar to the frequency reported at Mt. Daban on the northeastern TP in the post-monsoon season (80 %) (Du et al., 2015). The frequency at the Nam Co station during the pre-monsoon season was lower than that at NCO-P (38 %) (Venzac et al., 2008) and comparable with that at Mt. Yulong on the southeastern TP (14 %) (Shang et al., 2018) in the same season. In addition, the NPF frequencies of other high-altitude sites, such as Mt. Tai (Lv et al., 2018), Jungfraujoch (Tröstl et al., 2016b), Maïdo Observa-

https://doi.org/10.5194/acp-23-4343-2023

Table 1. Comparison of particle number concentration (PN) and NPF parameters (NPF frequency, CS, J, GR) with other high-altitude sites around the world.

Site	Altitude (m)	Observation date and season[a]	PN (cm^{-3})	NPF frequency	CS $\times 10^{-2}$ (s^{-1})	J ($cm^{-3}\,s^{-1}$)	GR ($nm\,h^{-1}$)	Reference
Nam Co station, China	4379	May 2019, pre-monsoon	$PN_{3-700} = 1163 \pm 1026$	15 %	0.14 ± 0.07	$J_4 = 1.11 \pm 0.79$	$GR_{4-25} = 4.2 \pm 0.9$	This study
		June 2019 monsoon	$PN_{3-700} = 3647 \pm 2671$	80 %	0.15 ± 0.05	$J_4 = 1.08 \pm 0.21$	$GR_{4-25} = 3.8 \pm 0.8$	
NCO-P[b], Nepal	5079	April–June 2007, pre-monsoon	NA	38 %	NA	$J_{10} = 0.14$	$GR = 1.8 \pm 0.7$	Venzac et al. (2008)
		July–September 2007, monsoon	NA	57 %	NA	$J_{10} = 0.19$	NA	
Mt. Daban, China	3295	September–October 2013, post-monsoon	$PN_{12-478} = 2400$	80 %	NA	NA	GR = 2.0	Du et al. (2015)
Mt. Yulong, China	3410	May–April 2015, pre-monsoon	$PN_{3-10\,000} = 1600 \pm 1290$	14 %	0.2	$J_3 = 1.18$	3.2	Shang et al. (2018)
Mt. Tai, China	1534	July–August 2014, summer	NA	21 %	1.1–4.8	$J_3 = 1.33$–52.54	$GR_{3-20} = 1.15$–7.76	Lv et al. (2018)
Jungfraujoch, Switzerland	3580	July 2013–June 2014, one year	$PN_{10-600} = 200$–1000	20 %	NA	$J_{3.2} = 0.2$–7.5	$GR_{5-15} = 4 \pm 2.3$	Tröstl et al. (2016b)
Maïdo Observatory, Réunion	2165	2015, one year	NA	67 %	0.02–2	$J_2 = 0.5$–30	$GR_{12-19} = 8$–45	Rose et al. (2019)
Storm Peak Laboratory, USA	3210	March–May 2001–2009, spring	NA	56 %	0.12 ± 0.05	$J_8 = 0.39 \pm 0.05$	$GR = 7.5 \pm 4.5$	Hallar et al. (2011)
		June–July 2001–2009, summer	NA	43 %	0.13 ± 0.06	$J_8 = 1.19 \pm 0.34$	$GR = 9.1 \pm 6.9$	

[a] The seasons in Tibet sites were divided into the pre-monsoon, monsoon and post-monsoon. The seasons not in the Tibet sites were divided into spring, summer, autumn and winter. [b] Nepal Climate Observatory at Pyramid site. NA: data not found in the literature.

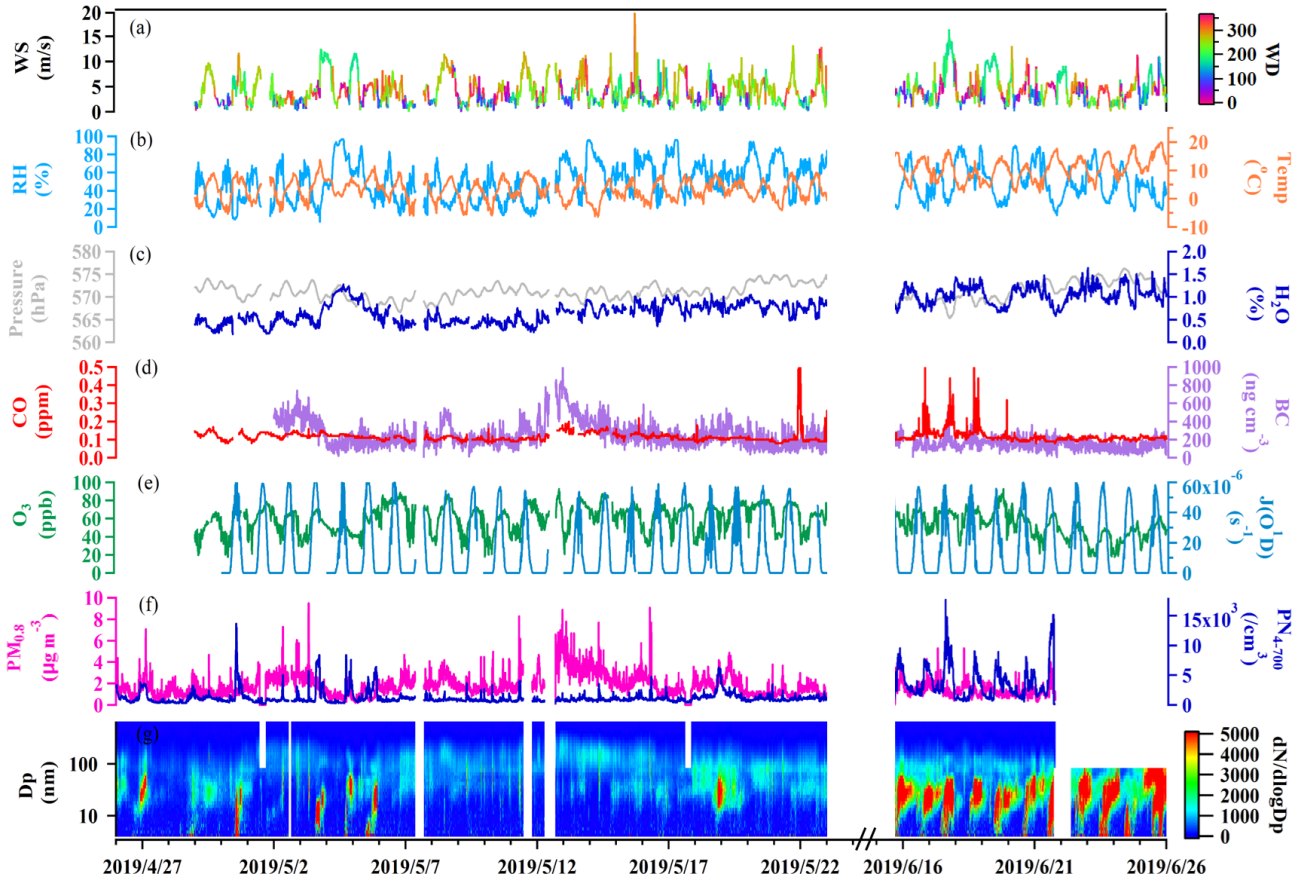

Figure 2. Time series during pre-monsoon and monsoon: **(a)** the wind speed and wind direction, **(b)** the ambient temperature and the relative humidity (RH), **(c)** the pressure and water content (H_2O) in air, **(d)** CO concentration and the black carbon (BC) concentration, **(e)** O_3 concentration and the photolysis frequencies of O_3 (JO^1D), **(f)** the $PM_{0.8}$ mass concentration and the number concentration of particles in size of 4–700 nm (PN_{4-700}), **(g)** the particle number size distributions (PNSDs).

tory (Rose et al., 2019) and Storm Peak Laboratory (Hallar et al., 2011), were basically between those in the pre-monsoon and monsoon seasons of the Nam Co station. In general, the frequencies of the two seasons at the Nam Co station can represent the highest and lowest values of NPF frequencies observed in the TP and other high-altitude sites, and even various environments (such as urban, rural, etc.) (Nieminen et al., 2018).

Table 1 summarizes the formation rate (J), growth rate (GR), and condensation sink (CS) at the Nam Co station and other high-altitude sites. The J_4 at the Nam Co station varied from 0.38 to 2.43 $cm^{-3}\,s^{-1}$, with an average value of $1.15 \pm 0.58\ cm^{-3}\,s^{-1}$, which is comparable with the results at Mt. Yulong (J_3, 1.18 $cm^{-3}\,s^{-1}$) (Shang et al., 2018) and Jungfraujoch ($J_{3.2}$, 0.2–7.5 $cm^{-3}\,s^{-1}$) (Tröstl et al., 2016b). However, the J at the Nam Co station was higher than the values at NCO-P site (J_{10}, 0.14–0.19 $cm^{-3}\,s^{-1}$) (Venzac et al., 2008) and Storm Peak Laboratory (J_8, 0.39-1.19 $cm^{-3}\,s^{-1}$) (Hallar et al., 2011), but lower than that at Mt. Tai (J_3, 1.33–52.54 $cm^{-3}\,s^{-1}$) (Lv et al., 2018) and Maïdo Observatory (J_2, 0.5–30 $cm^{-3}\,s^{-1}$) (Rose et al., 2019), which may be due to the distinction of particle size range used in the calculation and precursor concentrations between the sites. For example, SO_2 at Mt. Tai (3.2 ppb) (Lv et al., 2018) was much higher than that at Mt. Yulong (0.06 ppb) (Shang et al., 2018). The average GR in the size range of 4–25 nm at the Nam Co station varied from 1.5 to 5.6 $nm\,h^{-1}$, with the average value of $4.0 \pm 1.2\ nm\,h^{-1}$, which is comparable with those at Mt. Yulong (3.2 $nm\,h^{-1}$) (Shang et al., 2018) and Jungfraujoch (4.0 $nm\,h^{-1}$) (Tröstl et al., 2016b), and higher than those at NCO-P site ($1.8 \pm 0.7\ nm\,h^{-1}$) (Venzac et al., 2008) and Mt. Daban (2.0 $nm\,h^{-1}$) (Du et al., 2015), but lower than that at Maïdo Observatory (8–45 $nm\,h^{-1}$) (Rose et al., 2019). The average CS was $0.0015 \pm 0.0007\ s^{-1}$ at the Nam Co station, which is comparable with those at Mt. Yulong (0.0002 s^{-1}) (Shang et al., 2018), Maïdo Observatory (0.0002–0.02 s^{-1}) (Rose et al., 2019) and Storm Peak Laboratory (0.0012 s^{-1}) (Hallar et al., 2011), and much lower than that at Mt. Tai (0.011–0.048 s^{-1}) (Lv et al., 2018). In a word, the J, GR, and CS at the Nam Co station were within average levels in the high-altitude sites. Meanwhile, there was no significant variation in J, GR and daily CS between the pre-monsoon

and monsoon seasons, although the NPF frequencies of the two seasons were quite different. The key factors determining the occurrence of NPF events need to be further studied.

3.3 Frequent NPF events driven by summer monsoon

Whether an NPF event can occur is mainly related to (1) the CS, which mainly referred to the scavenging rate of precursors, clusters, and newly formed particles by background aerosols. High CS can lead to the continual reduction in newly formed particle number concentration and inhibit the occurrence of NPF, (2) the gaseous precursors that can participate in nucleation and growth, including sulfuric acid (Kulmala et al., 2013), dimethylamine (Yao et al., 2018), ammonia (Xiao et al., 2015) and VOC (Tröstl et al., 2016a; Fang et al., 2020; Qiao et al., 2021). A sufficiently high concentration of low-volatility vapors (precursors) can contribute to persistent nucleation and generating new atmospheric particles; (3) air mass origins and meteorological factors including WD, RH, temperature, the intensity of solar radiation, etc, which can influence the occurrence and intensity of NPF events by directly or indirectly affecting the source and sink parameters.

In the following, those potential reasons will be examined. For clarity, NPF event days occurring in the pre-monsoon and monsoon seasons were named NPF-pre days and NPF-monsoon days, respectively. Non-event days in the pre-monsoon season were termed non-event days, as non-event days in the monsoon season were scarce.

3.3.1 Condensation sink

CS is the key factor controlling the occurrence of NPF events especially in urban environment (Yan et al., 2021). At some high-altitude observations at a larger scale, the important role of the transported pre-existing particles in NPF events was also emphasized (Rose et al., 2019; Boulon et al., 2010). Here we analyzed the CS levels in NPF days and non-event days at the Nam Co station. As shown in Fig. 3a, the levels of CS in NPF-pre days, NPF-monsoon days and non-event days were approximate during 11:00–18:00 GMT+8 (the occurrence time of NPF events), although the CS in the early morning of NPF-pre days seems to be slightly lower. The CS was mainly in the range of 0.001–0.0015 s^{-1} during the NPF occurrence time, which was much lower than that at most locations in China, such as $\sim 0.01\ s^{-1}$ in urban Beijing (Deng et al., 2021), and 0.001–0.284 s^{-1} at Mt. Tai (Lv et al., 2018), and comparable with that at Mt. Yulong (0.002 s^{-1}) (Shang et al., 2018). The result varied from previous studies which reported much lower CS during NPF days than that in non-event days (Zhou et al., 2021; Lv et al., 2018). It indicated that CS was not the decisive factor controlling the occurrence of NPF events at the Nam Co station.

3.3.2 Gas precursors

Gaseous sulfuric acid is identified as the key precursor for nucleation and initial growth due to its low volatility (Kulmala et al., 2013; Qiao et al., 2021). Nucleation based on sulfuric acid and stabilizing species, such as ammonia and amines, is regarded as the dominant NPF mechanism in urban and rural environments. However, the role of gaseous sulfuric acid in NPF events may not be significant at the Nam Co station. The concentration of sulfuric acid in the atmosphere is related to the degree of SO_2, photochemical oxidation rate and CS. On the one hand, the level of SO_2 was considered to be comparable between NPF days and non-event days or maybe higher in non-event days. The SO_2 concentration was not measured directly in the observation periods, and the WRF/CMAQ-modeled SO_2 concentration was employed for analysis. It can be found that the modeled SO_2 concentration in the area was at a very low level, with the average value of 0.03 ± 0.02 ppb (Fig. S14), which was comparable with that measured at Mt. Yulong (Shang et al., 2018). For NPF and non-event days, slightly higher modeled SO_2 concentration was observed on non-event days and NPF-pre days compared with those on NPF-monsoon days. It indicates that the level of SO_2 may be related to the seasonal influence, and there is no significant difference between NPF days and non-event days. On the other hand, the photochemical oxidation intensities of SO_2 and CS were comparable between NPF days and non-event days. The photochemical oxidation intensity of SO_2 was indicated by J (O^1D). As shown in Fig. 3b, NPF-pre days, NPF-monsoon days and non-event days shared the same level of J (O^1D) (3×10^{-5}–$6 \times 10^{-5}\ s^{-1}$) during the occurrence time of NPF events. The CS levels were close among those three types of days as introduced in Sect. 3.3.1. With speculated comparable/lower SO_2 concentrations and similar CS and J (O^1D) levels, the abundance of gaseous sulfuric acid in NPF days would be approaching or a little lower than that on non-event days. In any case, it indicated that sulfuric acid may not govern the occurrence of NPF events at Nam Co station.

In addition to sulfuric acid, organics are also considered to be an important factor of NPF events. Observations and laboratory experiments have found that organics may participate in or even dominate the nucleation and growth process in NPF events in pristine environments and the preindustrial atmosphere. For example, CLOUD (Cosmics Leaving Outdoor Droplets) experiments observed obvious NPF events from highly oxidized organics without the involvement of sulfuric acid (Kirkby et al., 2016). At the high-altitude sites of Jungfraujoch and Himalaya, NPF events occurred mainly through the condensation of highly oxygenated molecules (HOMs) (Bianchi et al., 2016, 2021). Due to instrument status, VOC measurement was only available in the pre-monsoon season. The concentration of VOC (total VOC) showed a higher value (20 %) during 11:00–18:00 on NPF-pre days compared with non-event days (Fig. 3c). Aromatics,

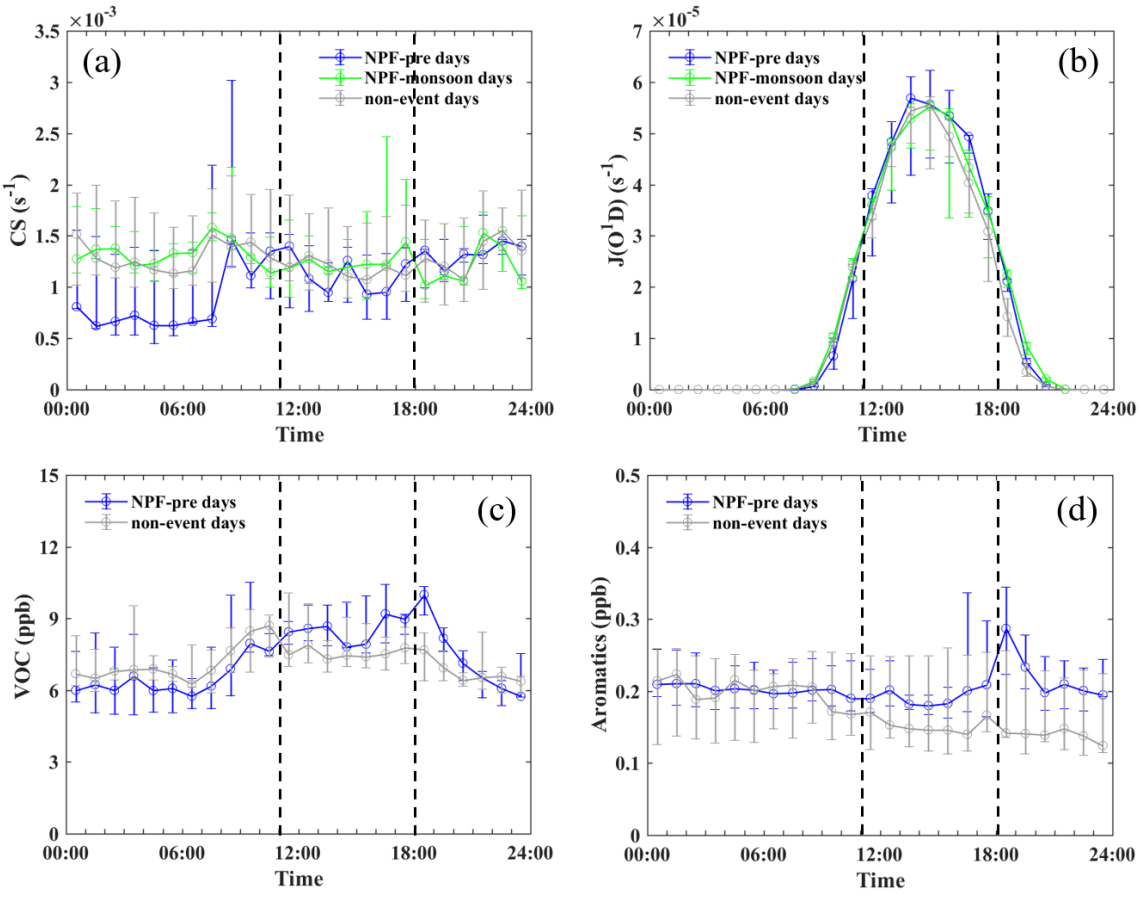

Figure 3. Diurnal variations of **(a)** condensation sink (CS), **(b)** JO^1D, the total concentration of **(c)** VOC and **(d)** aromatics in NPF-pre days, NPF-monsoon days and non-event days. The upper and lower bars indicate the 75th and 25th percentiles; the markers are the average values.

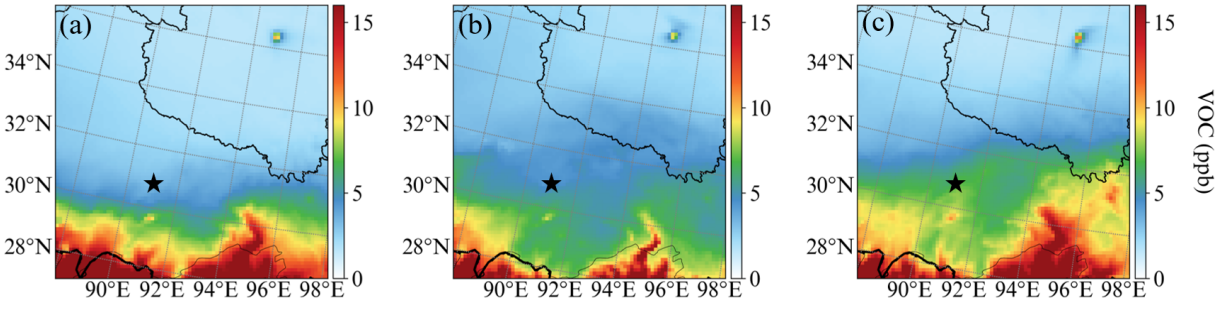

Figure 4. Model spatial distribution of VOC during **(a)** non-event days, **(b)** NPF-pre days and **(c)** NPF-monsoon days. The star is the Nam Co station.

which can be used as the indicator of anthropogenic emissions, also exhibited a higher level (20 %) during NPF-pre days (Fig. 3d). The aromatics have been considered to contribute substantially to new particle formation (Molteni et al., 2018). The potential NPF precursors such as toluene (Garmash et al., 2020), styrene (Yu et al., 2022) and trimethylbenzene (Molteni et al., 2018) showed higher values in NPF-pre days compared with those in non-event days (Fig. S15). This suggested that VOC such as aromatics may be the key factor in determining the occurrence of NPF events. In order to further evaluate the role of VOC, we used WRF/CMAQ models to simulate the spatial distribution of VOC concentration in the pre-monsoon and monsoon seasons. The detailed information about the model setting and evaluation can be found in Sect. S2. As shown in Fig. 4, the simulated VOC levels in NPF days including NPF-pre and NPF-monsoon days were higher than those in non-event days. The average modeled VOC concentrations in NPF-pre days and

NPF-monsoon days were 25 % and 88 % higher than those in non-event days, respectively. Therefore, we further considered that the organic matter could be the key factor to determine whether NPF event occurred. Nucleation of pure organics or organics involved could be the dominant mechanism at the Nam Co station. In addition, higher organic concentrations were observed in the monsoon season (NPF-monsoon days) compared with that in the pre-monsoon season (NPF-pre days and non-event days). The result is consistent with one recent study which has found that the concentration of monoterpene-derived HOMs in East Asia was higher in summer (June–August) than that in Spring (March–May) by using GEOS-Chem global chemical transport model (Xu et al., 2022). This means that the frequent NPF events in the monsoon season could be caused by the higher organic matters.

3.3.3 Air mass origins and meteorology

While the concentrations of organic precursors could be the most probable reasons for the occurrence of NPF events, the external factors driving the difference in VOC levels between the NPF and non-event days and other conditions that may affect the characteristics of NPF were still unknown. This indicated that a further investigation into other NPF-related variables was still required.

There are almost no local anthropogenic source emissions at the Nam Co station. Air pollutants at the observation site are mainly brought by air mass transmission. Backward trajectories were utilized to identify the air mass origins associated with NPF events. The frequencies of the 48 h back trajectories of air masses arriving at the Nam Co station during the occurrence time of nucleation (11:00–18:00) in non-event days, NPF-pre days and NPF-monsoon days are presented in Fig. 5. It can be found that the dominant air masses on non-event days were from the west (almost 100 %) and passed by western Nepal, northwestern India and Pakistan. In comparison, air masses in NPF-pre days and NPF-monsoon days mainly come from the south and southwest (57 % and 75 %) and originated in the northeastern India. WD, which can reflect the local situation for air masses and the source of air pollutants, showed a high frequency of strong southerly wind on NPF-pre days and NPF-monsoon days and westerly wind on non-event days (Fig. S16). The example of the spatial distribution of wind field in non-event days, NPF-pre days and NPF-monsoon days displayed the similar phenomenon on a larger scale (Fig. S17). These results suggested that the occurrence of NPF events was related to the southerly and southwesterly air masses. When the southerly air mass occurred, it may bring organic precursors from the southern region (northeastern India) to the Nam Co station, driving the occurrence of NPF events in this area. As for the significantly higher NPF frequency in the monsoon season, it resulted from the more frequent southerly air masses (summer monsoon) in the monsoon season in comparison with the pre-monsoon season as introduced in Sect. 3.1. The summer monsoon can bring the higher organic concentrations in the monsoon season (NPF-monsoon days) compared with those in the pre-monsoon season (NPF-pre and non-event days) (Fig. 4), thus triggering almost daily NPF events. A similar result was found in the recent study which showed that the Indian summer monsoon acted as a facilitator for transporting gaseous pollutants (Yin et al., 2021).

In Fig. 6, we show the diurnal variations of meteorological factors during NPF-pre days, NPF-monsoon days and non-event days at the Nam Co station. The temperatures on NPF-pre days and non-event days were generally close, but the temperature on NPF-monsoon days was obviously higher. The similar temperature on NPF-pre days and non-event days suggests that temperature is not a crucial factor for NPF event occurrence. Previous studies have found that higher temperature can increase the formation rate of HOMs but reduce the volatility of HOMs in the meantime. The effect of temperature on the nucleation rate may not be important in a limited ambient temperature range (Stolzenburg et al., 2018). But the higher temperature during NPF-monsoon days may promote biogenic VOC emissions, which favored particle nucleation and growth (Andreae et al., 2022). This may partly explain the phenomenon for the higher modeled VOC concentration on NPF-monsoon days than NPF-pre days. The average RH was similar on both NPF days and non-event days, although NPF-pre days had a wide range of RH changes. Laboratory studies have shown that water vapor can suppress the formation of extremely low volatility organic compounds (ELVOCs) from monoterpenes (Bonn et al., 2002). However, our result was the opposite. During 11:00–18:00, the water content (H_2O) in the air during NPF-monsoon days was the highest, NPF-pre days was the second, and non-event days was the lowest. This indicated the inhibition effect of water vapor was not important at the Nam Co station. The similar finding was also observed at remote sites in the subboreal forest of North America (Andreae et al., 2022).

Overall, our results are most consistent with the organics-involved nucleation mechanism. Condensation sink and gaseous sulfuric acid could have no significant effect on the occurrence of NPF events. The frequent NPF events in the summer monsoon season may result from the higher frequency of southerly and southwesterly air masses, which brought the organic precursors to participate in the NPF process.

3.4 Significant increase of CCN in the monsoon season

The CCN concentration was estimated following the method introduced in Sect. 2.5. Considering the similar proportions of chemical components between the Nam Co station and Mt. Yulong with around 70 % fraction of organics, and the stability of the fractions of chemical components (J. Xu et al., 2018) (Shang et al., 2018), the hygroscopicity parameter κ was assumed to be equal to 0.12 throughout the measurement period according to the previous measurement at

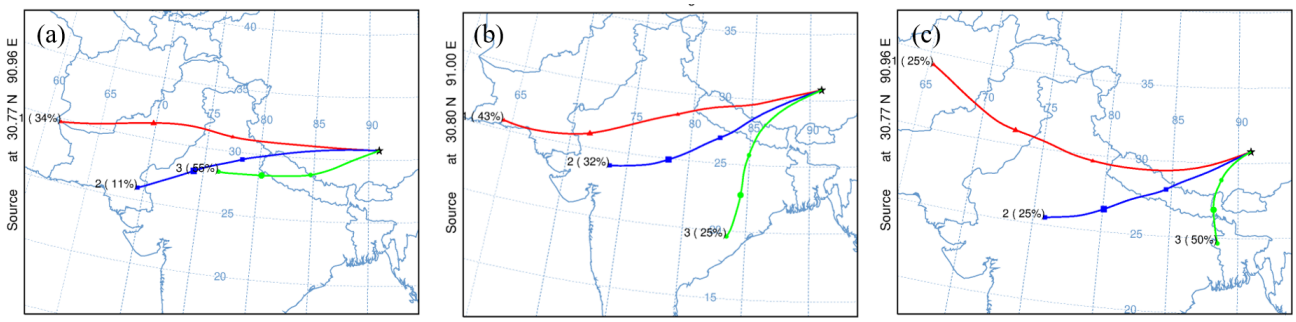

Figure 5. The frequencies of the 48 h back trajectories of air masses arriving at the Nam Co station from different directions during the occurrence time of nucleation (11:00–18:00) in **(a)** non-event days, **(b)** NPF-pre days and **(c)** NPF-monsoon days.

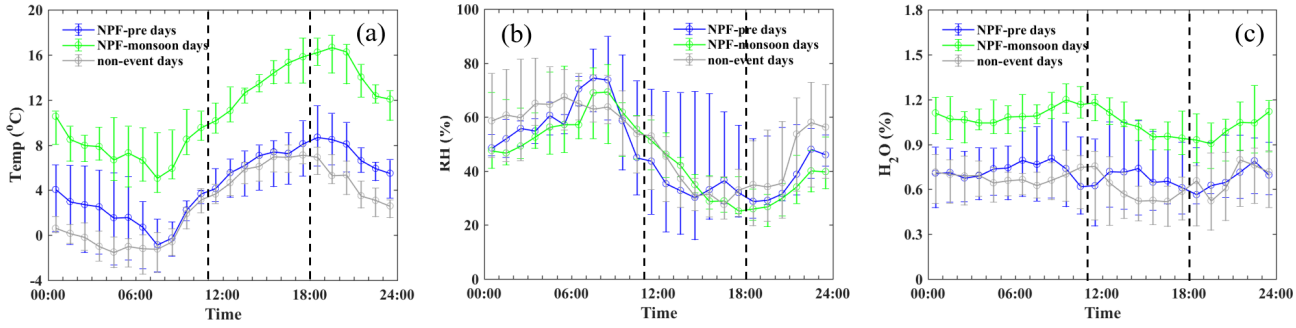

Figure 6. Diurnal variations of **(a)** temperature, **(b)** RH and **(c)** the water content (H_2O) in the air on NPF-pre days, NPF-monsoon days and non-event days. The upper and lower bars indicate the 75th and 25th percentiles; the markers are the average values.

Mt. Yulong in the TP (Shang et al., 2018). As a result, the D_c values at S_c levels of 0.6 % and 1.2 % were 73.4 ± 1.3 and 46.3 ± 0.8 nm, respectively. No noticeable difference in D_c was found between the pre-monsoon and monsoon seasons ($S_c = 0.6$ %: 74.4 ± 1.0 vs. 72.4 ± 1.1 nm, $S_c = 1.2$ %: 46.9 ± 0.6 vs. 45.7 ± 0.7 nm). There could be uncertainties in the values of κ due to the variation of chemical components, but they had little impact on D_c and thus on the final result of CCN concentration.

The high-frequency NPF events in the summer monsoon period markedly increased the number concentration of atmospheric aerosols. The average PNSDs during the pre-monsoon and monsoon seasons are plotted in Fig. 7a with much higher number concentrations observed during the monsoon season. The mean total particle number concentration (PN_{4-700}) in the monsoon season was 3647 ± 2671 cm^{-3}, which was more than 2 times higher than that of the pre-monsoon season (1163 ± 1026 cm^{-3}). Although the measured particle size ranges were not the same as other studies, the results can still be comparable as the background particles were mainly distributed in tens to hundreds of nanometers. As shown in Table 1, PN_{4-700} at the Nam Co station in the pre-monsoon season was comparable with other high-altitude sites around the world, while PN_{4-700} in the monsoon season was much higher due to the frequent NPF events. The atmospheric particles contributed by new particle nucleation and growth in the monsoon season were mainly concentrated below 100 nm. Among them, the concentration of nucleation mode particles (4–25 nm) in the monsoon season was about 2 times higher than that in the pre-monsoon season, and the concentration of Aitken mode particles (25–100 nm) was 3.5 times higher than that in the pre-monsoon season. In contrast, accumulation mode particles (> 100 nm) which were related to the secondary formation process (Wang et al., 2013), were nearly at the same level in the two seasons (around 200 cm^{-3}). As for CCN, the average number concentrations of CCN at S_c of 0.6 % and 1.2 % in the monsoon season were 434 ± 242 and 863 ± 628 cm^{-3}, respectively (Fig. 8). The results were about 0.1 and 0.6 times higher than those in the pre-monsoon season at S_c of 0.6 % (396 ± 177 cm^{-3}) and 1.2 % (552 ± 261 cm^{-3}).

In addition to the average particle number concentration in the two seasons, the important impact of NPF events is more reflected in the increased number concentration of aerosol and CCN within a few hours after particle nucleation and growth, that is, the aerosol and CCN production. The aerosol production and CCN production during one day can be obtained by comparing the particle number concentration at the beginning of the increase of the target particles (N_{init}) with the maximum number concentration (N_{max}), as introduced by Rose et al. (2017). The N_{init} and N_{max} are hourly average concentrations as shown in Fig. S18. Figure 9 shows the aver-

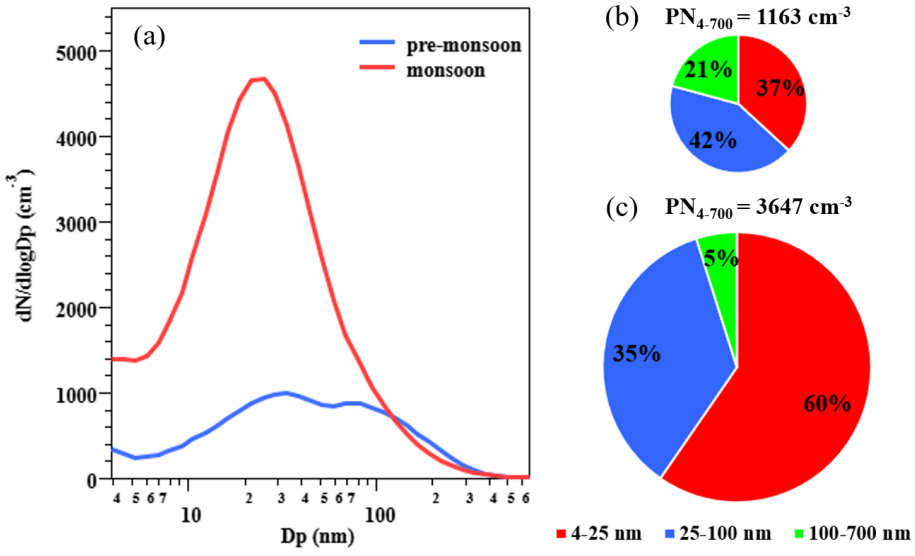

Figure 7. Particle number size distribution (PNSD) at the Nam Co station. **(a)** Mean PNSD in pre-monsoon and monsoon; the contribution of different size ranges (4–25 nm, 25–100 nm, 100–700 nm) to the total particle number concentration **(b)** in pre-monsoon and **(c)** in monsoon.

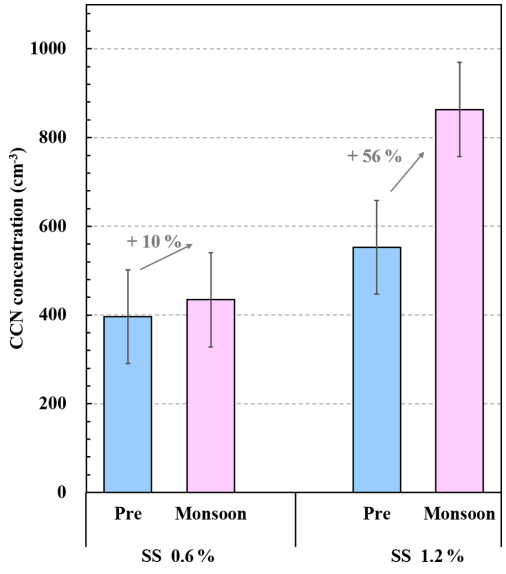

Figure 8. Mean number concentration of CCN at S_c of 0.6 % and 1.2 % in the pre-monsoon and monsoon seasons.

age daily variation of PNSD, three-mode particles and CCN in the whole period in the pre-monsoon season and monsoon season. Higher daily aerosol production and CCN production were observed during the monsoon season compared with those in the pre-monsoon season. In the monsoon season, nucleation mode particles (4–25 nm) started to increase quickly at around 11:00 when nucleation occurred. The freshly nucleated particles grew to larger sizes due to condensation and coagulation of the pre-existing particles within several hours, which contributed to the increase of Aitken mode particles (25–100 nm) from 15:00. The average daily aerosol production of nucleation mode particles and Aitken mode particles in the monsoon season was around 3400 and 1200 cm^{-3}, respectively. As for CCN, the average production of CCN at S_c of 0.6 % and 1.2 % in the monsoon season was 180 and 518 cm^{-3}, respectively. The production of CCN were lower than previous studies because they only considered NPF days and their environment was relatively polluted (Rose et al., 2017; Shen et al., 2016). The production of aerosols and CCN was much lower in the pre-monsoon season, although the particles and CCN at around 11:00 were comparable with the monsoon season. The average daily aerosol production of nucleation mode particles and Aitken mode particles in the pre-monsoon season were around 500 and 300 cm^{-3}, respectively. And the CCN production at S_c of 0.6 % and 1.2 % was 160 and 286 cm^{-3}, respectively. The average daily production of nucleation mode particles, Aitken mode particles and CCN at S_c of 1.2 % in the monsoon season was 5.8, 3 and 0.8 times higher than that in the pre-monsoon season, respectively.

It should be noted that the CCN concentration and production we estimated above were local ground levels, which can be considered as the minimum values. That is because those smaller particles (< 40 nm) formed by NPF may further grow and reach CCN size on the following days during transportation, as the coagulation sink affecting the lifetime of aerosols was at a low level. This mechanism was verified at different high-altitude stations such as NCO-P site, Chacaltaya and Jungfraujoch (Venzac et al., 2008; Rose et al., 2015; Tröstl et al., 2016b). The nucleation mode and Aitken mode particle bands in the morning reflected the continuation of NPF events. As a result, the amount of potential CCN in the monsoon season could be much larger than the result measured here, due to the high level of the smaller particles.

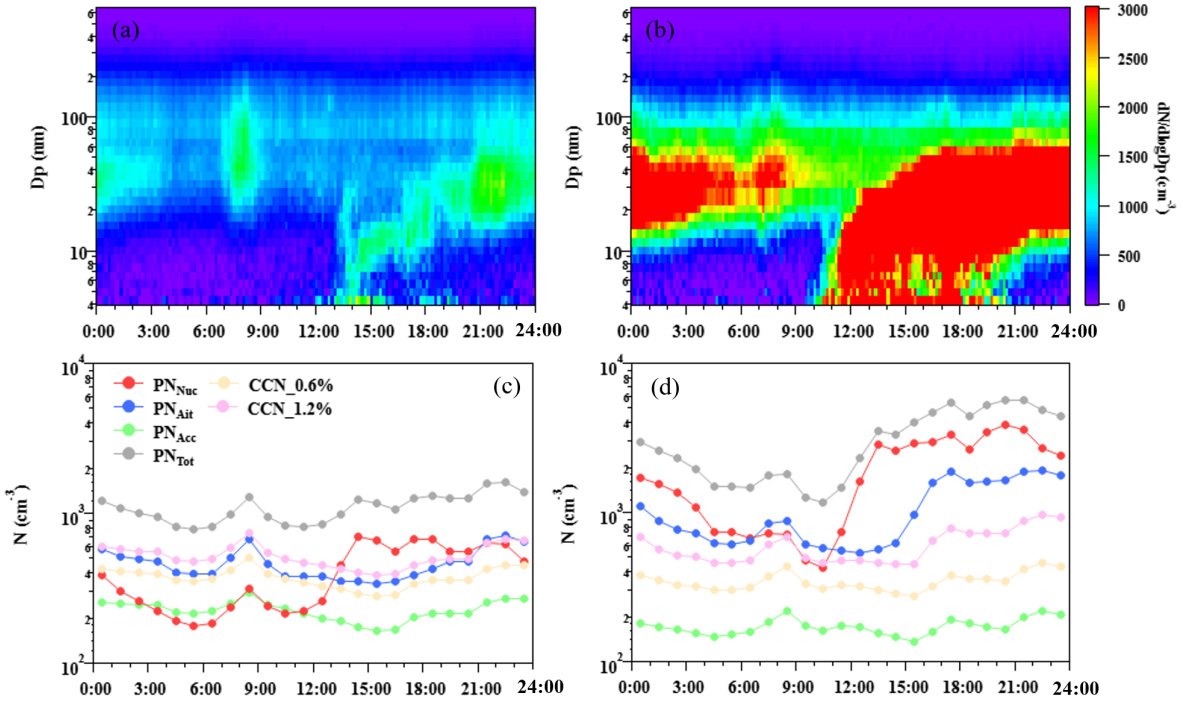

Figure 9. Diurnal variations of particle number size distributions (PNSDs) and the number concentrations of nucleation mode particles (PN_{Nuc}), Aitken mode particles (PN_{Ait}), accumulation mode particles (PN_{Acc}), the total particles (PN_{Tot}), CCN at S_c of 0.6 % (CCN_0.6 %) and 1.2 % (CCN_1.2 %) during the pre-monsoon **(a, c)** and monsoon **(b, d)** seasons.

Therefore, the climate effect from aerosols may have a large variance between the pre-monsoon and monsoon season.

4 Summary and conclusions

The PNSDs, trace gases and meteorological parameters were measured at the Nam Co station (4730 m a.s.l.) in the central Tibetan Plateau (TP) during the pre-monsoon and summer monsoon seasons. Firstly, meteorological conditions between the pre-monsoon and monsoon seasons were distinct with higher temperature and water content in the monsoon season. Strong westerlies pass through western Nepal, northwestern India and Pakistan in the pre-monsoon season, while air masses were mainly derived from the south (Bangladesh and northeastern India) in the monsoon period. Secondly, as the pristine high-altitude site, low levels of particles and gaseous pollutants were displayed at the Nam Co station. Relatively higher pollutant concentration was found during the pre-monsoon season due to less favorable atmospheric circulation.

The most important finding of this study was that there were evident seasonal differences in the frequencies of NPF events at the Nam Co station with 15 % in the pre-monsoon season and 80 % in the monsoon season, which can represent the lowest and highest values of NPF frequencies observed in the TP and other high-altitude sites, even around the world. In addition, there was no noticeable variation in J, GR, and CS between the pre-monsoon and monsoon seasons at the Nam Co station. Although the measured precursors were limited at our sites, the comprehensive analysis of the measured CS, gaseous precursors and meteorological conditions, supplemented by the modeled SO_2 and VOC, points to the organic involved nucleation as the dominant mechanism. Condensation sink and gaseous sulfuric acid could have no significant effect on the occurrence of NPF events. The frequent NPF events in the summer monsoon season may result from the higher frequency of southerly and southwesterly air masses, which brought the organic precursors to participate in the NPF process.

The frequent NPF events in the summer monsoon season had elevated the number concentration of atmospheric aerosols and CCN at the Nam Co station. The average total particle number concentration in the monsoon season was more than 2 times higher than that in the pre-monsoon season, mainly contributed by nucleation mode and Aitken mode particles. And the average number concentrations of CCN at S_c of 0.6 % and 1.2 % in the monsoon season were 0.1 and 0.6 times higher than those in the pre-monsoon season. As for aerosol and CCN production, the average daily production of nucleation mode particles, Aitken mode particles and CCN at S_c of 1.2 % in the monsoon season was 5.8, 3 and 0.8 times higher than that in the pre-monsoon season, respectively. Considering that the smaller particles (< 40 nm) formed by NPF may further grow and reach CCN size dur-

ing the following days due to the low-level coagulation sink, the amount of potential CCN in the monsoon season could be much larger than our local measurement results. It may markedly affect the earth's radiation balance and global climate. Our results emphasized that seasonal effect of NPF should be considered in model simulations when calculating the amounts of aerosols and CCN in high-altitude atmosphere. Long-term measurement campaigns with a more comprehensive set of instrumentation to investigate the role of NPF in high-altitude atmosphere are required for a deeper scientific understanding of NPF process and its role in the global aerosol budget.

Data availability. The data provided in this paper can be obtained from the author upon request (minhu@pku.edu.cn).

Supplement. The supplement related to this article is available online at: https://doi.org/10.5194/acp-23-4343-2023-supplement.

Author contributions. LT: investigation, data curation, methodology, formal analysis, writing – original draft, writing – review and editing. MH: project administration, supervision, funding acquisition, writing – review and editing. DS: investigation, data curation, methodology, formal analysis. XF: investigation, data curation, methodology, formal analysis. JM: investigation, data curation. WX: data curation. JZ: data curation. WZ: data curation. YW: data curation. CZ: data curation. YZ: data curation. JH: data curation. LZ: data curation. CY: project administration, funding acquisition, data curation. SG: writing – review and editing. ZW: writing – review and editing.

Competing interests. The contact author has declared that none of the authors has any competing interests.

Disclaimer. Publisher's note: Copernicus Publications remains neutral with regard to jurisdictional claims in published maps and institutional affiliations.

Special issue statement. This article is part of the special issue "In-depth study of the atmospheric chemistry over the Tibetan Plateau: measurement, processing, and the impacts on climate and air quality (ACP/AMT inter-journal SI)". It is not associated with a conference.

Acknowledgements. The research has been supported by the National Natural Science Foundation of China (grant nos. 91844301 and 91544214), National Research Program for Key Issues in Air Pollution Control (grant no. DQGG0103), National Key Research and Development Program of China (grant no. 2016YFC0202000: Task 3), and the second Tibetan Plateau Scientific Expedition and Research Program (STEP, grant no. 2019QZKK0606).

Financial support. The research has been supported by the National Natural Science Foundation of China (grant nos. 91844301 and 91544214), National Research Program for Key Issues in Air Pollution Control (grant no. DQGG0103), National Key Research and Development Program of China (grant no. 2016YFC0202000: Task 3), and the second Tibetan Plateau Scientific Expedition and Research Program (STEP, grant no. 2019QZKK0606).

Review statement. This paper was edited by Markku Kulmala and reviewed by three anonymous referees.

References

Andreae, M. O., Andreae, T. W., Ditas, F., and Pöhlker, C.: Frequent new particle formation at remote sites in the subboreal forest of North America, Atmos. Chem. Phys., 22, 2487–2505, https://doi.org/10.5194/acp-22-2487-2022, 2022.

Appel, K. W., Bash, J. O., Fahey, K. M., Foley, K. M., Gilliam, R. C., Hogrefe, C., Hutzell, W. T., Kang, D., Mathur, R., Murphy, B. N., Napelenok, S. L., Nolte, C. G., Pleim, J. E., Pouliot, G. A., Pye, H. O. T., Ran, L., Roselle, S. J., Sarwar, G., Schwede, D. B., Sidi, F. I., Spero, T. L., and Wong, D. C.: The Community Multiscale Air Quality (CMAQ) model versions 5.3 and 5.3.1: system updates and evaluation, Geosci. Model Dev., 14, 2867–2897, https://doi.org/10.5194/gmd-14-2867-2021, 2021.

Bianchi, F., Tröstl, J., Junninen, H., Frege, C., Henne, S., Hoyle, C. R., Molteni, U., Herrmann, E., Adamov, A., Bukowiecki, N., Chen, X., Duplissy, J., Gysel, M., Hutterli, M., Kangasluoma, J., Kontkanen, J., Kürten, A., Manninen, H. E., Münch, S., Peräkylä, O., Petäjä, T., Rondo, L., Williamson, C., Weingartner, E., Curtius, J., Worsnop, D. R., Kulmala, M., Dommen, J., and Baltensperger, U.: New particle formation in the free troposphere: A question of chemistry and timing, Science, 352, 1109–1112, https://doi.org/10.1126/science.aad5456, 2016.

Bianchi, F., Junninen, H., Bigi, A., Sinclair, V. A., Dada, L., Hoyle, C. R., Zha, Q., Yao, L., Ahonen, L. R., Bonasoni, P., Buenrostro Mazon, S., Hutterli, M., Laj, P., Lehtipalo, K., Kangasluoma, J., Kerminen, V. M., Kontkanen, J., Marinoni, A., Mirme, S., Molteni, U., Petäjä, T., Riva, M., Rose, C., Sellegri, K., Yan, C., Worsnop, D. R., Kulmala, M., Baltensperger, U., and Dommen, J.: Biogenic particles formed in the Himalaya as an important source of free tropospheric aerosols, Nat. Geosci., 14, 4–9, https://doi.org/10.1038/s41561-020-00661-5, 2021.

Bonasoni, P., Laj, P., Marinoni, A., Sprenger, M., Angelini, F., Arduini, J., Bonafè, U., Calzolari, F., Colombo, T., Decesari, S., Di Biagio, C., di Sarra, A. G., Evangelisti, F., Duchi, R., Facchini, M. C., Fuzzi, S., Gobbi, G. P., Maione, M., Panday, A., Roccato, F., Sellegri, K., Venzac, H., Verza, G. P., Villani, P., Vuillermoz, E., and Cristofanelli, P.: Atmospheric Brown Clouds in the Himalayas: first two years of continuous observations at the Nepal Climate Observatory-Pyramid (5079 m), Atmos. Chem. Phys., 10, 7515–7531, https://doi.org/10.5194/acp-10-7515-2010, 2010.

Bonn, B., Schuster, G., and Moortgat, G. K.: Influence of Water Vapor on the Process of New Particle Formation during Monoterpene Ozonolysis, J. Phys. Chem. A, 106, 2869–2881, https://doi.org/10.1021/jp012713p, 2002.

Boulon, J., Sellegri, K., Venzac, H., Picard, D., Weingartner, E., Wehrle, G., Collaud Coen, M., Bütikofer, R., Flückiger, E., Baltensperger, U., and Laj, P.: New particle formation and ultrafine charged aerosol climatology at a high altitude site in the Alps (Jungfraujoch, 3580 m a.s.l., Switzerland), Atmos. Chem. Phys., 10, 9333–9349, https://doi.org/10.5194/acp-10-9333-2010, 2010.

Cai, R. and Jiang, J.: A new balance formula to estimate new particle formation rate: reevaluating the effect of coagulation scavenging, Atmos. Chem. Phys., 17, 12659–12675, https://doi.org/10.5194/acp-17-12659-2017, 2017.

Chen, S., Wang, H., Lu, K., Zeng, L., Hu, M., and Zhang, Y.: The trend of surface ozone in Beijing from 2013 to 2019: Indications of the persisting strong atmospheric oxidation capacity, Atmos. Environ., 242, 117801, https://doi.org/10.1016/j.atmosenv.2020.117801, 2020.

Cong, Z., Kang, S., Kawamura, K., Liu, B., Wan, X., Wang, Z., Gao, S., and Fu, P.: Carbonaceous aerosols on the south edge of the Tibetan Plateau: concentrations, seasonality and sources, Atmos. Chem. Phys., 15, 1573–1584, https://doi.org/10.5194/acp-15-1573-2015, 2015.

Dal Maso, M., Kulmala, M., Riipinen, I., and Wagner, R.: Formation and growth of fresh atmospheric aerosols: Eight years of aerosol size distribution data from SMEAR II, Hyytiälä, Finland, Boreal Environ. Res., 10, 323–336, 2005.

Deng, C., Cai, R., Yan, C., Zheng, J., and Jiang, J.: Formation and growth of sub-3 nm particles in megacities: impact of background aerosols, Faraday Discuss., 226, 348–363, https://doi.org/10.1039/D0FD00083C, 2021.

Du, W., Sun, Y. L., Xu, Y. S., Jiang, Q., Wang, Q. Q., Yang, W., Wang, F., Bai, Z. P., Zhao, X. D., and Yang, Y. C.: Chemical characterization of submicron aerosol and particle growth events at a national background site (3295 m a.s.l.) on the Tibetan Plateau, Atmos. Chem. Phys., 15, 10811–10824, https://doi.org/10.5194/acp-15-10811-2015, 2015.

Fang, X., Hu, M., Shang, D., Tang, R., Shi, L., Olenius, T., Wang, Y., Wang, H., Zhang, Z., Chen, S., Yu, X., Zhu, W., Lou, S., Ma, Y., Li, X., Zeng, L., Wu, Z., Zheng, J., and Guo, S.: Observational Evidence for the Involvement of Dicarboxylic Acids in Particle Nucleation, Environ. Sci. Technol. Lett., 7, 388–394, https://doi.org/10.1021/acs.estlett.0c00270, 2020.

Garmash, O., Rissanen, M. P., Pullinen, I., Schmitt, S., Kausiala, O., Tillmann, R., Zhao, D., Percival, C., Bannan, T. J., Priestley, M., Hallquist, Å. M., Kleist, E., Kiendler-Scharr, A., Hallquist, M., Berndt, T., McFiggans, G., Wildt, J., Mentel, T. F., and Ehn, M.: Multi-generation OH oxidation as a source for highly oxygenated organic molecules from aromatics, Atmos. Chem. Phys., 20, 515–537, https://doi.org/10.5194/acp-20-515-2020, 2020.

Gordon, H., Kirkby, J., Baltensperger, U., Bianchi, F., Breitenlechner, M., Curtius, J., Dias, A., Dommen, J., Donahue, N. M., Dunne, E. M., Duplissy, J., Ehrhart, S., Flagan, R. C., Frege, C., Fuchs, C., Hansel, A., Hoyle, C. R., Kulmala, M., Kürten, A., Lehtipalo, K., Makhmutov, V., Molteni, U., Rissanen, M. P., Stozkhov, Y., Tröstl, J., Tsagkogeorgas, G., Wagner, R., Williamson, C., Wimmer, D., Winkler, P. M., Yan, C., and Carslaw, K. S.: Causes and importance of new particle formation in the present-day and preindustrial atmospheres, J. Geophys. Res.-Atmos., 122, 8739–8760, https://doi.org/10.1002/2017JD026844, 2017.

Guenther, A. B., Jiang, X., Heald, C. L., Sakulyanontvittaya, T., Duhl, T., Emmons, L. K., and Wang, X.: The Model of Emissions of Gases and Aerosols from Nature version 2.1 (MEGAN2.1): an extended and updated framework for modeling biogenic emissions, Geosci. Model Dev., 5, 1471–1492, https://doi.org/10.5194/gmd-5-1471-2012, 2012.

Hallar, A. G., Lowenthal, D. H., Chirokova, G., Borys, R. D., and Wiedinmyer, C.: Persistent daily new particle formation at a mountain-top location, Atmos. Environ., 45, 4111–4115, https://doi.org/10.1016/j.atmosenv.2011.04.044, 2011.

Hu, J., Wang, P., Ying, Q., Zhang, H., Chen, J., Ge, X., Li, X., Jiang, J., Wang, S., Zhang, J., Zhao, Y., and Zhang, Y.: Modeling biogenic and anthropogenic secondary organic aerosol in China, Atmos. Chem. Phys., 17, 77–92, https://doi.org/10.5194/acp-17-77-2017, 2017.

IPCC: Climate Change 2021: The Physical Science Basis. Contribution of Working Group I to the Sixth Assessment Report of the Intergovernmental Panel on Climate Change, edited by: Masson-Delmotte, V., Zhai, P., Pirani, A., Connors, S. L., Péan, C., Berger, S., Caud, N., Chen, Y., Goldfarb, L., Gomis, M. I., Huang, M., Leitzell, K., Lonnoy, E., Matthews, J. B. R., Maycock, T. K., Waterfield, T., Yelekçi, O., Yu, R., and Zhou, B., Cambridge University Press, Cambridge, United Kingdom and New York, NY, USA, in press, https://doi.org/10.1017/9781009157896, 2021.

Kerminen, V.-M., Chen, X., Vakkari, V., Petäjä, T., Kulmala, M., and Bianchi, F.: Atmospheric new particle formation and growth: review of field observations, Environ. Res. Lett., 13, 103003, https://doi.org/10.1088/1748-9326/aadf3c, 2018.

Kirchstetter, T. W., Novakov, T., and Hobbs, P. V.: Evidence that the spectral dependence of light absorption by aerosols is affected by organic carbon, J. Geophys. Res.-Atmos., 109, D21208, https://doi.org/10.1029/2004jd004999, 2004.

Kirkby, J., Duplissy, J., Sengupta, K., Frege, C., Gordon, H., Williamson, C., Heinritzi, M., Simon, M., Yan, C., Almeida, J., Tröstl, J., Nieminen, T., Ortega, I. K., Wagner, R., Adamov, A., Amorim, A., Bernhammer, A.-K., Bianchi, F., Breitenlechner, M., Brilke, S., Chen, X., Craven, J., Dias, A., Ehrhart, S., Flagan, R. C., Franchin, A., Fuchs, C., Guida, R., Hakala, J., Hoyle, C. R., Jokinen, T., Junninen, H., Kangasluoma, J., Kim, J., Krapf, M., Kürten, A., Laaksonen, A., Lehtipalo, K., Makhmutov, V., Mathot, S., Molteni, U., Onnela, A., Peräkylä, O., Piel, F., Petäjä, T., Praplan, A. P., Pringle, K., Rap, A., Richards, N. A. D., Riipinen, I., Rissanen, M. P., Rondo, L., Sarnela, N., Schobesberger, S., Scott, C. E., Seinfeld, J. H., Sipilä, M., Steiner, G., Stozhkov, Y., Stratmann, F., Tomé, A., Virtanen, A., Vogel, A. L., Wagner, A. C., Wagner, P. E., Weingartner, E., Wimmer, D., Winkler, P. M., Ye, P., Zhang, X., Hansel, A., Dommen, J., Donahue, N. M., Worsnop, D. R., Baltensperger, U., Kulmala, M., Carslaw, K. S., and Curtius, J.: Ion-induced nucleation of pure biogenic particles, Nature, 533, 521–526, https://doi.org/10.1038/nature17953, 2016.

Kulmala, M., Kontkanen, J., Junninen, H., Lehtipalo, K., Manninen, H., Nieminen, T., Petäjä, T., Sipilä, M., Schobesberger, S., Rantala, P., Franchin, A., Jokinen, T., Järvinen,

E., Äijälä, M., Kangasluoma, J., Hakala, J., Aalto, P., Paasonen, P., Mikkilä, J., and Worsnop, D.: Direct Observations of Atmospheric Aerosol Nucleation, Science, 339, 943–946, https://doi.org/10.1126/science.1227385, 2013.

Lv, G., Sui, X., Chen, J., Jayaratne, R., and Mellouki, A.: Investigation of new particle formation at the summit of Mt. Tai, China, Atmos. Chem. Phys., 18, 2243–2258, https://doi.org/10.5194/acp-18-2243-2018, 2018.

Mao, J., Li, L., Li, J., Sulaymon, I. D., Xiong, K., Wang, K., Zhu, J., Chen, G., Ye, F., Zhang, N., Qin, Y., Qin, M., and Hu, J.: Evaluation of Long-Term Modeling Fine Particulate Matter and Ozone in China During 2013–2019, Front. Environ. Sci., 10, 872249, https://doi.org/10.3389/fenvs.2022.872249, 2022.

Merikanto, J., Spracklen, D. V., Mann, G. W., Pickering, S. J., and Carslaw, K. S.: Impact of nucleation on global CCN, Atmos. Chem. Phys., 9, 8601–8616, https://doi.org/10.5194/acp-9-8601-2009, 2009.

Molteni, U., Bianchi, F., Klein, F., El Haddad, I., Frege, C., Rossi, M. J., Dommen, J., and Baltensperger, U.: Formation of highly oxygenated organic molecules from aromatic compounds, Atmos. Chem. Phys., 18, 1909–1921, https://doi.org/10.5194/acp-18-1909-2018, 2018.

Nieminen, T., Kerminen, V.-M., Petäjä, T., Aalto, P. P., Arshinov, M., Asmi, E., Baltensperger, U., Beddows, D. C. S., Beukes, J. P., Collins, D., Ding, A., Harrison, R. M., Henzing, B., Hooda, R., Hu, M., Hõrrak, U., Kivekäs, N., Komsaare, K., Krejci, R., Kristensson, A., Laakso, L., Laaksonen, A., Leaitch, W. R., Lihavainen, H., Mihalopoulos, N., Németh, Z., Nie, W., O'Dowd, C., Salma, I., Sellegri, K., Svenningsson, B., Swietlicki, E., Tunved, P., Ulevicius, V., Vakkari, V., Vana, M., Wiedensohler, A., Wu, Z., Virtanen, A., and Kulmala, M.: Global analysis of continental boundary layer new particle formation based on long-term measurements, Atmos. Chem. Phys., 18, 14737–14756, https://doi.org/10.5194/acp-18-14737-2018, 2018.

Petters, M. D. and Kreidenweis, S. M.: A single parameter representation of hygroscopic growth and cloud condensation nucleus activity, Atmos. Chem. Phys., 7, 1961–1971, https://doi.org/10.5194/acp-7-1961-2007, 2007.

Qiao, X., Yan, C., Li, X., Guo, Y., Yin, R., Deng, C., Li, C., Nie, W., Wang, M., Cai, R., Huang, D., Wang, Z., Yao, L., Worsnop, D. R., Bianchi, F., Liu, Y., Donahue, N. M., Kulmala, M., and Jiang, J.: Contribution of Atmospheric Oxygenated Organic Compounds to Particle Growth in an Urban Environment, Environ. Sci. Technol., 55, 13646–13656, https://doi.org/10.1021/acs.est.1c02095, 2021.

Rose, C., Sellegri, K., Velarde, F., Moreno, I., Ramonet, M., Weinhold, K., Krejci, R., Ginot, P., Andrade, M., Wiedensohler, A., and Laj, P.: Frequent nucleation events at the high altitude station of Chacaltaya (5240 m a.s.l.), Bolivia, Atmos. Environ., 102, 18–29, https://doi.org/10.1016/j.atmosenv.2014.11.015, 2015.

Rose, C., Sellegri, K., Moreno, I., Velarde, F., Ramonet, M., Weinhold, K., Krejci, R., Andrade, M., Wiedensohler, A., Ginot, P., and Laj, P.: CCN production by new particle formation in the free troposphere, Atmos. Chem. Phys., 17, 1529–1541, https://doi.org/10.5194/acp-17-1529-2017, 2017.

Rose, C., Foucart, B., Picard, D., Colomb, A., Metzger, J.-M., Tulet, P., and Sellegri, K.: New particle formation in the volcanic eruption plume of the Piton de la Fournaise: specific features from a long-term dataset, Atmos. Chem. Phys., 19, 13243–13265, https://doi.org/10.5194/acp-19-13243-2019, 2019.

Shang, D., Hu, M., Zheng, J., Qin, Y., Du, Z., Li, M., Fang, J., Peng, J., Wu, Y., Lu, S., and Guo, S.: Particle number size distribution and new particle formation under the influence of biomass burning at a high altitude background site at Mt. Yulong (3410 m), China, Atmos. Chem. Phys., 18, 15687–15703, https://doi.org/10.5194/acp-18-15687-2018, 2018.

Shen, X., Sun, J., Zhang, X., Zhang, Y., Zhang, L., and Fan, R.: Key features of new particle formation events at background sites in China and their influence on cloud condensation nuclei, Front. Environ. Sci. Eng., 10, 5, https://doi.org/10.1007/s11783-016-0833-2, 2016.

Stolzenburg, D., Fischer, L., Vogel, A. L., Heinritzi, M., Schervish, M., Simon, M., Wagner, A. C., Dada, L., Ahonen, L. R., Amorim, A., Baccarini, A., Bauer, P. S., Baumgartner, B., Bergen, A., Bianchi, F., Breitenlechner, M., Brilke, S., Buenrostro Mazon, S., Chen, D., Dias, A., Draper, D. C., Duplissy, J., El Haddad, I., Finkenzeller, H., Frege, C., Fuchs, C., Garmash, O., Gordon, H., He, X., Helm, J., Hofbauer, V., Hoyle, C. R., Kim, C., Kirkby, J., Kontkanen, J., Kürten, A., Lampilahti, J., Lawler, M., Lehtipalo, K., Leiminger, M., Mai, H., Mathot, S., Mentler, B., Molteni, U., Nie, W., Nieminen, T., Nowak, J. B., Ojdanic, A., Onnela, A., Passananti, M., Petäjä, T., Quéléver, L. L. J., Rissanen, M. P., Sarnela, N., Schallhart, S., Tauber, C., Tomé, A., Wagner, R., Wang, M., Weitz, L., Wimmer, D., Xiao, M., Yan, C., Ye, P., Zha, Q., Baltensperger, U., Curtius, J., Dommen, J., Flagan, R. C., Kulmala, M., Smith, J. N., Worsnop, D. R., Hansel, A., Donahue, N. M., and Winkler, P. M.: Rapid growth of organic aerosol nanoparticles over a wide tropospheric temperature range, P. Natl. Acad. Sci. USA, 115, 9122–9127, https://doi.org/10.1073/pnas.1807604115, 2018.

Tröstl, J., Chuang, W. K., Gordon, H., Heinritzi, M., Yan, C., Molteni, U., Ahlm, L., Frege, C., Bianchi, F., Wagner, R., Simon, M., Lehtipalo, K., Williamson, C., Craven, J. S., Duplissy, J., Adamov, A., Almeida, J., Bernhammer, A.-K., Breitenlechner, M., Brilke, S., Dias, A., Ehrhart, S., Flagan, R. C., Franchin, A., Fuchs, C., Guida, R., Gysel, M., Hansel, A., Hoyle, C. R., Jokinen, T., Junninen, H., Kangasluoma, J., Keskinen, H., Kim, J., Krapf, M., Kürten, A., Laaksonen, A., Lawler, M., Leiminger, M., Mathot, S., Möhler, O., Nieminen, T., Onnela, A., Petäjä, T., Piel, F. M., Miettinen, P., Rissanen, M. P., Rondo, L., Sarnela, N., Schobesberger, S., Sengupta, K., Sipilä, M., Smith, J. N., Steiner, G., Tomè, A., Virtanen, A., Wagner, A. C., Weingartner, E., Wimmer, D., Winkler, P. M., Ye, P., Carslaw, K. S., Curtius, J., Dommen, J., Kirkby, J., Kulmala, M., Riipinen, I., Worsnop, D. R., Donahue, N. M., and Baltensperger, U.: The role of low-volatility organic compounds in initial particle growth in the atmosphere, Nature, 533, 527–531, https://doi.org/10.1038/nature18271, 2016a.

Tröstl, J., Herrmann, E., Frege, C., Bianchi, F., Molteni, U., Bukowiecki, N., Hoyle, C. R., Steinbacher, M., Weingartner, E., Dommen, J., Gysel, M., and Baltensperger, U.: Contribution of new particle formation to the total aerosol concentration at the high-altitude site Jungfraujoch (3580 m asl, Switzerland), J. Geophys. Res.-Atmos., 121, 11692–11711, https://doi.org/10.1002/2015JD024637, 2016b.

Venzac, H., Sellegri, K., Laj, P., Villani, P., Bonasoni, P., Marinoni, A., Cristofanelli, P., Calzolari, F., Fuzzi, S.,

Decesari, S., Facchini, M.-C., Vuillermoz, E., and Verza, G. P.: High frequency new particle formation in the Himalayas, P. Natl. Acad. Sci. USA, 105, 15666–15671, https://doi.org/10.1073/pnas.0801355105, 2008.

Wang, M., Zeng, L., Lu, S., Shao, M., Liu, X., Yu, X., Chen, W., Yuan, B., Zhang, Q., Hu, M., and Zhang, Z.: Development and validation of a cryogen-free automatic gas chromatograph system (GC-MS/FID) for online measurements of volatile organic compounds, Anal. Methods, 6, 9424–9434, https://doi.org/10.1039/C4AY01855A, 2014.

Wang, M., Xu, B., Wang, N., Cao, J., Tie, X., Wang, H., Zhu, C., and Yang, W.: Two distinct patterns of seasonal variation of airborne black carbon over Tibetan Plateau, Sci. Total Environ., 573, 1041–1052, https://doi.org/10.1016/j.scitotenv.2016.08.184, 2016.

Wang, Z. B., Hu, M., Wu, Z. J., Yue, D. L., He, L. Y., Huang, X. F., Liu, X. G., and Wiedensohler, A.: Long-term measurements of particle number size distributions and the relationships with air mass history and source apportionment in the summer of Beijing, Atmos. Chem. Phys., 13, 10159–10170, https://doi.org/10.5194/acp-13-10159-2013, 2013.

Wiedensohler, A., Birmili, W., Nowak, A., Sonntag, A., Weinhold, K., Merkel, M., Wehner, B., Tuch, T., Pfeifer, S., Fiebig, M., Fjäraa, A. M., Asmi, E., Sellegri, K., Depuy, R., Venzac, H., Villani, P., Laj, P., Aalto, P., Ogren, J. A., Swietlicki, E., Williams, P., Roldin, P., Quincey, P., Hüglin, C., Fierz-Schmidhauser, R., Gysel, M., Weingartner, E., Riccobono, F., Santos, S., Grüning, C., Faloon, K., Beddows, D., Harrison, R., Monahan, C., Jennings, S. G., O'Dowd, C. D., Marinoni, A., Horn, H.-G., Keck, L., Jiang, J., Scheckman, J., McMurry, P. H., Deng, Z., Zhao, C. S., Moerman, M., Henzing, B., de Leeuw, G., Löschau, G., and Bastian, S.: Mobility particle size spectrometers: harmonization of technical standards and data structure to facilitate high quality long-term observations of atmospheric particle number size distributions, Atmos. Meas. Tech., 5, 657–685, https://doi.org/10.5194/amt-5-657-2012, 2012.

Wiedinmyer, C., Akagi, S. K., Yokelson, R. J., Emmons, L. K., Al-Saadi, J. A., Orlando, J. J., and Soja, A. J.: The Fire INventory from NCAR (FINN): a high resolution global model to estimate the emissions from open burning, Geosci. Model Dev., 4, 625–641, https://doi.org/10.5194/gmd-4-625-2011, 2011.

Xiao, S., Wang, M. Y., Yao, L., Kulmala, M., Zhou, B., Yang, X., Chen, J. M., Wang, D. F., Fu, Q. Y., Worsnop, D. R., and Wang, L.: Strong atmospheric new particle formation in winter in urban Shanghai, China, Atmos. Chem. Phys., 15, 1769–1781, https://doi.org/10.5194/acp-15-1769-2015, 2015.

Xu, J., Zhang, Q., Shi, J., Ge, X., Xie, C., Wang, J., Kang, S., Zhang, R., and Wang, Y.: Chemical characteristics of submicron particles at the central Tibetan Plateau: insights from aerosol mass spectrometry, Atmos. Chem. Phys., 18, 427–443, https://doi.org/10.5194/acp-18-427-2018, 2018.

Xu, J., Hettiyadura, A. P. S., Liu, Y., Zhang, X., Kang, S., and Laskin, A.: Regional Differences of Chemical Composition and Optical Properties of Aerosols in the Tibetan Plateau, J. Geophys. Res.-Atmos., 125, e2019JD031226, https://doi.org/10.1029/2019JD031226, 2020.

Xu, R., Tie, X., Li, G., Zhao, S., Cao, J., Feng, T., and Long, X.: Effect of biomass burning on black carbon (BC) in South Asia and Tibetan Plateau: The analysis of WRF-Chem modeling, Sci. Total Environ., 645, 901–912, https://doi.org/10.1016/j.scitotenv.2018.07.165, 2018.

Xu, R., Thornton, J. A., Lee, B. H., Zhang, Y., Jaeglé, L., Lopez-Hilfiker, F. D., Rantala, P., and Petäjä, T.: Global simulations of monoterpene-derived peroxy radical fates and the distributions of highly oxygenated organic molecules (HOMs) and accretion products, Atmos. Chem. Phys., 22, 5477–5494, https://doi.org/10.5194/acp-22-5477-2022, 2022.

Yan, C., Yin, R., Lu, Y., Dada, L., Yang, D., Fu, Y., Kontkanen, J., Deng, C., Garmash, O., Ruan, J., Baalbaki, R., Schervish, M., Cai, R., Bloss, M., Chan, T., Chen, T., Chen, Q., Chen, X., Chen, Y., Chu, B., Dällenbach, K., Foreback, B., He, X., Heikkinen, L., Jokinen, T., Junninen, H., Kangasluoma, J., Kokkonen, T., Kurppa, M., Lehtipalo, K., Li, H., Li, H., Li, X., Liu, Y., Ma, Q., Paasonen, P., Rantala, P., Pileci, R. E., Rusanen, A., Sarnela, N., Simonen, P., Wang, S., Wang, W., Wang, Y., Xue, M., Yang, G., Yao, L., Zhou, Y., Kujansuu, J., Petäjä, T., Nie, W., Ma, Y., Ge, M., He, H., Donahue, N. M., Worsnop, D. R., Kerminen, V.-M., Wang, L., Liu, Y., Zheng, J., Kulmala, M., Jiang, J., and Bianchi, F.: The Synergistic Role of Sulfuric Acid, Bases, and Oxidized Organics Governing New-Particle Formation in Beijing, Geophys. Res. Lett., 48, e2020GL091944, https://doi.org/10.1029/2020GL091944, 2021.

Yanai, M. and Wu, G.-X.: Effects of the Tibetan Plateau, in: The Asian Monsoon, edited by: Wang, B., Springer Berlin Heidelberg, Berlin, Heidelberg, 513–549, https://doi.org/10.1007/3-540-37722-0_13, 2006.

Yao, L., Garmash, O., Bianchi, F., Zheng, J., Yan, C., Kontkanen, J., Junninen, H., Mazon, S., Ehn, M., Paasonen, P., Sipilä, M., Wang, M., Wang, X., Xiao, S., Chen, H., Lu, Y., Zhang, B., Wang, D., Fu, Q., and Wang, L.: Atmospheric new particle formation from sulfuric acid and amines in a Chinese megacity, Science, 361, 278–281, https://doi.org/10.1126/science.aao4839, 2018.

Yin, X., Kang, S., Foy, B. d., Rupakheti, D., Rupakheti, M., Cong, Z., Wan, X., Zhang, G., and Zhang, Q.: Impacts of Indian summer monsoon and stratospheric intrusion on air pollutants in the inland Tibetan Plateau, Geosci. Front., 12, 101255, https://doi.org/10.1016/j.gsf.2021.101255, 2021.

Yu, S., Jia, L., Xu, Y., and Pan, Y.: Formation of extremely low-volatility organic compounds from styrene ozonolysis: Implication for nucleation, Chemosphere, 305, 135459, https://doi.org/10.1016/j.chemosphere.2022.135459, 2022.

Zhang, X., Xu, J., Kang, S., Sun, J., Shi, J., Gong, C., Sun, X., Du, H., Ge, X., and Zhang, Q.: Regional Differences in the Light Absorption Properties of Fine Particulate Matter Over the Tibetan Plateau: Insights From HR-ToF-AMS and Aethalometer Measurements, J. Geophys. Res.-Atmos., 126, e2021JD035562, https://doi.org/10.1029/2021JD035562, 2021.

Zhou, Y., Hakala, S., Yan, C., Gao, Y., Yao, X., Chu, B., Chan, T., Kangasluoma, J., Gani, S., Kontkanen, J., Paasonen, P., Liu, Y., Petäjä, T., Kulmala, M., and Dada, L.: Measurement report: New particle formation characteristics at an urban and a mountain station in northern China, Atmos. Chem. Phys., 21, 17885–17906, https://doi.org/10.5194/acp-21-17885-2021, 2021.